^{119}Sn spin-lattice relaxation in α-SnF_2

Guenther Neue,[1] Shi Bai,[2] Robert E. Taylor,[3] Peter A. Beckmann,[2,4] Alexander J. Vega,[2] and Cecil Dybowski[2]
[1]*Physical Chemistry, TU Dortmund, D-44221 Dortmund, Germany*
[2]*Department of Chemistry and Biochemistry, University of Delaware, Newark, Delaware 19716, USA*
[3]*Department of Chemistry and Biochemistry, University of California at Los Angeles, Los Angeles, California 90095, USA*
[4]*Department of Physics, Bryn Mawr College, Bryn Mawr, Pennsylvania 19010, USA*
(Received 23 April 2009; revised manuscript received 14 May 2009; published 19 June 2009)

The temperature and magnetic field dependencies of the ^{119}Sn nuclear spin-lattice relaxation rate in α-SnF_2 indicate the presence of two relaxation mechanisms. At temperatures below 350 K, the relaxation is dominated by a nuclear spin-rotation interaction modulated by lattice vibrations, as has been seen for Pb and Tl salts. This ^{119}Sn relaxation pathway is less effective in SnF_2 than it is for ^{207}Pb, ^{203}Tl, and ^{205}Tl relaxation in some Pb and Tl salts but it is more effective than ^{111}Cd and ^{113}Cd relaxation in some Cd salts. Above 350 K, there is an additional contribution to the observed relaxation rate. The most likely candidate for this thermally activated contribution is the modulation of the ^{119}Sn-^{19}F dipolar interaction by fluoride-ion motion.

DOI: 10.1103/PhysRevB.79.214302 PACS number(s): 66.30.Dn, 76.60.−k, 61.72.Hh, 82.56.Na

I. INTRODUCTION

^{207}Pb nuclear spin-lattice relaxation in $Pb(NO_3)_2$,[1,2] $PbMoO_4$,[2,3] $PbCl_2$,[3] $PbTiO_3$,[4] and ^{203}Tl and/or ^{205}Tl nuclear spin-lattice relaxation in $TlNO_3$,[5] $TlClO_4$,[6] and $TlNO_2$ (Ref. 7) have been shown to arise from the Raman scattering of phonons by the Pb or Tl nuclei.[8] The mechanism was proposed for solid ^{129}Xe by Fitzgerald *et al.*[9] and expanded by Vega *et al.*[8] Treated semiclassically, the mechanism involves the random modulation of a local magnetic spin-rotation field caused by the relative rotational motions of neighboring atoms participating in lattice vibrations. Whereas the usual mechanism of spin-rotation relaxation involves modulation of a well-defined angular momentum of a molecule or an atomic group by collisions in a gas,[10] angular momentum is not a meaningful parameter for the solid materials under investigation here. Instead, the nuclear spin-rotation interaction responsible for the relaxation in these spin-$\frac{1}{2}$ metal salts is characterized by the modulation of the relative angular *velocity*. The modulation of the angular velocity *and* the interatomic distance of an atom pair gives rise to a Raman mechanism. The Raman process, though well known for spin relaxation of quadrupolar nuclei (spin $I>\frac{1}{2}$),[11,12] was unexpected for spin-$\frac{1}{2}$ nuclei.[13]

To understand this unusual and unexpected relaxation pathway for heavy spin-$\frac{1}{2}$ nuclei better, we have investigated other heavy spin-$\frac{1}{2}$ systems. This mechanism is not dominant (i.e., not observable) for ^{111}Cd and ^{113}Cd (both spin-$\frac{1}{2}$) spin-lattice relaxation in $CdMoO_4$ (Ref. 14) or in CdI_2.[15] In the present work, we report measurements of the ^{119}Sn (spin-$\frac{1}{2}$) spin-lattice relaxation rate constant R in SnF_2 between 238 and 420 K. ($R=1/T_1$, where T_1 is the nuclear spin-lattice relaxation time.) The Raman nuclear spin-rotation relaxation pathway is dominant at the lower end of the temperature range but at higher temperatures an additional thermally activated ^{119}Sn relaxation mechanism appears. While we cannot, unequivocally, specify the physical origin of the relaxation, fluoride-ion motion that modulates the ^{119}Sn-^{19}F nuclear spin-spin dipolar interaction seems the most likely candidate.

Stannous fluoride, SnF_2, exists in three forms: α-SnF_2 which is the thermodynamically stable form below 423 K, β-SnF_2 which is metastable below 340 K, and γ-SnF_2 which is stable between 423 and 483 K.[16] The kinetics of transformation among these phases is complex, involving changes over a range of temperatures and conditions[17] that may affect the relaxation of tin nuclei at temperatures in this regime. The crystal is monoclinic, with space group $C2/c$, containing 16 SnF_2 units per unit cell.[16,18] There are two inequivalent tin atoms and four inequivalent fluorine atoms in the unit cell as shown in Fig. 1. The structure is often described as containing four Sn_4F_8 tetramers, but this description is somewhat artificial. Within the four tetramers Sn-F distances range from 0.205 to 0.228 nm.

α-SnF_2 exhibits thermally activated electrical conductivity on the order of 10^{-7} S cm^{-1} at room temperature, which increases to $\sim 10^{-4}$ S cm^{-1} near the $\alpha \rightarrow \gamma$ phase transition at 423 K. The electronic contribution is less than 3%, so the conductivity is mediated almost exclusively by F^- ion

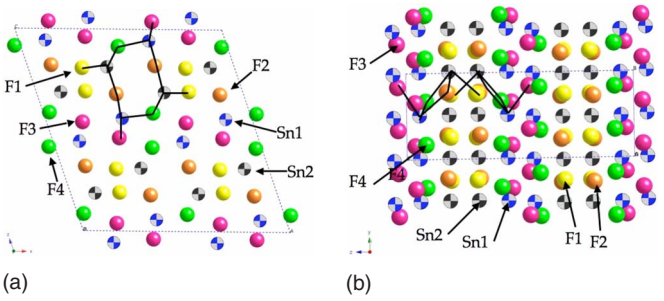

FIG. 1. (Color online) The crystal structure of α-SnF_2. There are two inequivalent Sn sites as indicated (blue and black colored beach balls online) and there are four inequivalent F sites as indicated (four different solid colors online). The tetramer Sn_4F_8 is indicated by solid lines. (a) The (010) plane based on Fig. 2 of Ref. 16. (b) The (100) plane based on Fig. 3 of Ref. 16. The same tetramer is indicated in both parts. There are four such tetramers in the unit cell, which is indicated. The structure was taken from the inorganic structure database (Ref. 19) and the figure was made using CRYSTALMAKER.

movement.[16] Many solid-state fluoride-ion conductors are based on the incorporation of SnF_2 in matrices with other metal fluorides, producing such technologically important materials as $SnF_2 \cdot PbF_2$ and $2SnF_2 \cdot NH_4F$.[20] A recent review lists the properties of several SnF_2-based materials and discusses the influence of impurities and mechanical defects in such materials.[21] Some F^- ion conductors have been studied with solid-state nuclear magnetic resonance (NMR) techniques.[22–27] However, to our knowledge, similar studies of single component SnF_2 have not yet been done. The present work on the nuclear spin-lattice relaxation of ^{119}Sn at higher temperatures provides an estimate of an effective activation energy. Interpreting this activation energy as one that characterizes F^- ion movement results in general agreement with conductivity measurements in the literature.[16]

II. EXPERIMENTAL PROCEDURE AND RESULTS

The polycrystalline sample of SnF_2 was purchased from Sigma-Aldrich and was used as received. The quoted purity was 99%. Crystallinity and purity of the SnF_2 were checked by x-ray powder diffraction. The material is overwhelmingly well-crystallized α-SnF_2, with small traces of a material that appears to be an oxide. The trace impurities exhibit quite sharp peaks in the x-ray spectrum, implying that they are in large associations spatially separated from the α-SnF_2. Presumably, the trace oxide phases are located at the surfaces of crystals, where they form a passivation layer that prevents further degradation by air and moisture.[28] Moreover, neither static nor magic angle spinning ^{119}Sn NMR spectrum shows any signals that can be identified as the signature of a tin oxide under the conditions at which relaxation measurements were performed. We conclude from these facts that the tin in the α-SnF_2 in this material relaxes independently of the presence of this oxidic component.

The temperature dependence of the ^{119}Sn nuclear spin-lattice relaxation rate constant R was measured at 74.6 MHz on a Tecmag Discovery NMR spectrometer in a magnetic field of 4.695 T. The $\pi/2$ pulse width was 4.0 μs. Measurements of R were also carried out at 111.9 MHz on a Bruker AVANCE DSX-300 spectrometer having a magnetic field of 7.049 T. The $\pi/2$ pulse width was 3.0 μs.

The ^{119}Sn NMR spectrum, shown in Fig. 2, reflects the significant chemical-shielding anisotropy in this material. The spectrum consists of two overlapping powder spectra corresponding to the two Sn sites (Fig. 1). The spectrum is referenced to the resonance of neat $Sn(CH_3)_4$ (δ=0 ppm) via the absolute frequency determined by comparison to the frequency of the carbon resonance of $Si(CH_3)_4$ in the same magnetic field.[29] There are few reported NMR spectra of solid Sn(II) compounds.[30]

In determining nuclear spin-lattice relaxation rate constants R, magnetization-recovery curves at both $\omega_{Sn}/2\pi$ =74.6 and 111.9 MHz were observed using a saturation-recovery procedure. Typically, a train of 20 closely spaced $\pi/2$ pulses was followed by a variable delay, t, after which the signal was detected with the spin-echo sequence using spin-temperature alternation. The pulse sequence is[3,31]

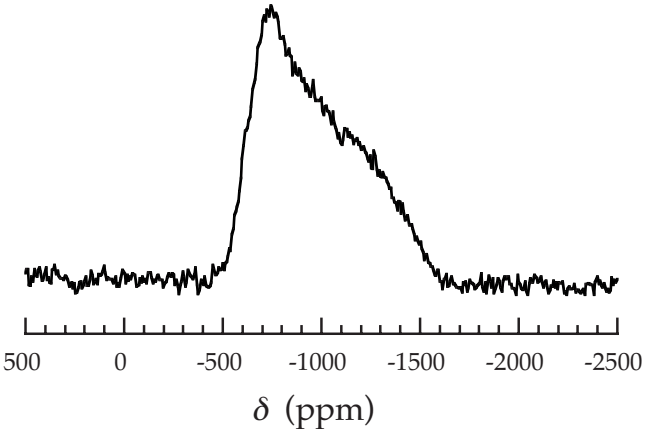

FIG. 2. The ^{119}Sn NMR spectrum of a polycrystalline sample of SnF_2 at 295 K and 74.6 MHz.

$$\{\pi/2 - \tau_4 - \pi/2 - \tau_4 \cdots \pi/2\} - t - \{\pi/2 - \tau_1 - \pi\} - \tau_2 - \text{acquire}(+) - \tau_5 -$$
$$\{\pi/2 - \tau_4 - \pi/2 - \tau_4 \cdots \pi/2\} - t - \{\pi - \tau_3 - \pi/2 - \tau_1 - \pi\} - \tau_2 - \text{acquire}(-) - \tau_5 - ,$$

with τ_4 set to about 5 μs, τ_3 set to about 1 ms, τ_1 set to about 20 μs, τ_2 set to start the acquisition at the exact time of the spin echo (typically about 20 μs), and τ_5 set to about 100 ms. The relaxation was always found to be exponential within experimental uncertainty and the relaxation was uniform across the line shape. The recovery of magnetization in this saturation-recovery experiment is

$$M(t) = M(\infty)[1 - e^{-Rt}], \tag{1}$$

where $M(t)$ is the magnetization, $M(\infty)$ is the equilibrium magnetization, and $R(=1/T_1)$ is the relaxation rate constant.

Temperature regulation above room temperature (296 K) was achieved by blowing heated nitrogen gas over the sample. Sample temperatures at, or lower than, room temperature (296 K) were achieved using a vortex-tube cooling device.[32] Temperature was measured by monitoring the chemical-shift difference in the proton spectrum of ethylene glycol $[OH(CH_2)_2OH]$ (Refs. 33 and 34) or by monitoring the chemical shift of a static $Pb(NO_3)_2$ sample.[35]

Figure 3 shows the temperature dependence of the ^{119}Sn spin-lattice relaxation rate constant R from 238 to 420 K at $\omega_{Sn}/2\pi$=74.6 and 111.9 MHz. The data in the lower temperature range are consistent with the Raman mechanism. We plot R versus T^2 in Fig. 3 to indicate that at the lower temperatures,

$$R = AT^2, \tag{2}$$

with A independent of magnetic field (i.e., independent of nuclear Larmor frequency ω_{Sn}), in agreement with the Raman contribution to the nuclear spin-rotation relaxation mechanism.[8] The data extrapolated to low temperature have an intercept of zero within experimental uncertainty, which also agrees with the predictions of the model. Fitting the low-temperature data gives $A=(2.21 \pm 0.02) \times 10^{-7}$ s^{-1} K^{-2}, and this temperature dependence is shown as the straight line

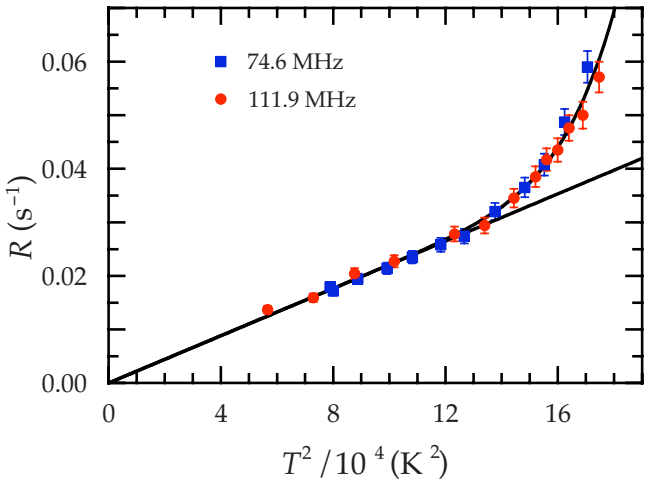

FIG. 3. (Color online) The ^{119}Sn spin-lattice relaxation rate constant, R, in SnF_2 as a function of T^2 at 74.6 and 111.9 MHz. The straight line is given by Eq. (2) and the top line is given by Eqs. (2) and (3), both with parameters given in the text.

in Fig. 3. Figure 4 shows the difference $R' = R - AT^2$ for the high-temperature data, plotted according to an Arrhenius equation. The linearity suggests that this difference relaxation is due to a thermally activated mechanism,

$$R' = B \exp\left(-\frac{E}{kT}\right). \tag{3}$$

This relaxation process is frequency dependent, as is evident from the divergence of the relaxation rate constants at the highest temperatures. Separate linear least-squares fits ($\ln R'$ versus T^{-1}) to the two sets of data, shown in Fig. 4, give $E = 64 \pm 4$ kJ mol^{-1} and $\ln(B/\mathrm{s}^{-1}) = 14 \pm 1$ for 111.9 MHz, and $E = 76 \pm 3$ kJ mol^{-1} and $\ln(B/\mathrm{s}^{-1}) = 18 \pm 1$ for 74.6 MHz. The fit considering all data together yields $E = 68 \pm 4$ kJ mol^{-1} and $\ln(B/\mathrm{s}^{-1}) = 15 \pm 1$. All three fits are shown in Fig. 4. The total temperature dependence $R = AT^2 + B \exp(-E/kT)$ is shown in Fig. 3, where mean values of $E = 70$ kJ mol^{-1} and $\ln(B/\mathrm{s}^{-1}) = 16$ were used to construct the line. Considering all these fits, we take the apparent activation energy of the relaxation process to be 70 ± 10 kJ mol^{-1}.

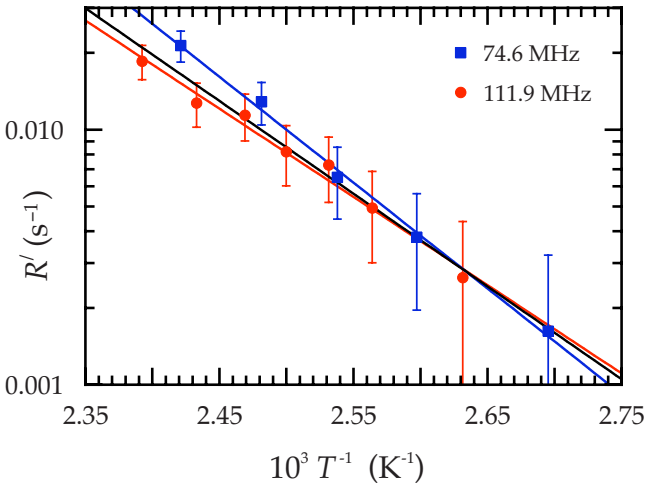

FIG. 4. (Color online) The difference between the observed relaxation rates and the AT^2 term (the straight line in Fig. 3) in Eq. (2). The straight lines are given by Eq. (3) for the 74.6 MHz data, the 111.9 MHz data, and both data sets taken as one, with parameters given in the text.

III. DISCUSSION

The temperature and magnetic field dependencies of the ^{119}Sn spin-lattice relaxation rate constants measured at lower temperatures in α-SnF_2 are consistent with a model whereby the relaxation involves *only* the nuclear spin-rotation relaxation process[8] and the observed relaxation rate constants at higher temperatures involve, *in addition*, a contribution from a thermally activated process.

The theoretical basis for relaxation by the spin-rotation process is the connection of the fluctuations of the local nuclear spin-rotation magnetic field $B_{\mathrm{local}}(t)$ to the time dependence (due to random lattice vibrations) of *both* the angular velocity $\Omega(t)$ of a vector connecting the nucleus to a nearest-neighbor atom and the deviations of the length $a + d(t)$ of this vector from its equilibrium value a.[8] The local field and the angular velocity are related through a proportionality coefficient Γ that depends on the interatomic distance as described by

$$B_{\mathrm{local}} = \Gamma\Omega = \Gamma_0(1 - \varepsilon d)\Omega, \tag{4}$$

where Γ_0 is the magnetorotation constant[8] and the parameter ε is related to the spatial derivative of Γ evaluated at the equilibrium interatomic separation. Simultaneous fluctuations of $\Omega(t)$ and $d(t)$ give rise to a Raman spin-relaxation process. Using the semiclassical model for relaxation and assuming a Debye model for the lattice vibrations in these crystals,[8] A in Eq. (2) is given by

$$A = \frac{2\pi\sqrt{2}\gamma^2 a^2 \varepsilon^2 \Gamma_0^2 k^3 \Theta_D}{7\hbar m^2 v^4}, \tag{5}$$

where k is Boltzmann's constant, γ is the magnetogyric ratio of the ^{119}Sn nucleus, Θ_D is the Debye temperature, m is the average atomic mass in the solid material, v is the speed of sound, and the other parameters have been introduced previously.

The fact that $\Omega(t)$ and $d(t)$ are mainly driven by transverse and longitudinal lattice vibrations, respectively, has significance for the conventional description of the Raman nuclear spin-lattice relaxation mechanism as a quantum-mechanical phonon-scattering process, whereby each spin flip is accompanied by the creation of one phonon and the simultaneous annihilation of another phonon. In the model that leads to the relaxation rate constant given by Eq. (2) [with Eq. (5)], one of these is a transverse-mode phonon, whereas the other is a longitudinal-mode phonon.[8] Other vibration-mode combinations, such as a transverse mode causing angular-velocity modulation and another transverse mode causing modulation of Γ through bond-angle fluctuations, also contribute to the relaxation mechanism but were not considered explicitly. We expect that distance modulations have a more pronounced effect.[8]

TABLE I. Raman relaxation coefficients for various materials.

Material	Nucleus	$10^6 A$ (s^{-1} K^{-2})	$10^{22} A/\gamma^2$ (s T^2 K^{-2})	Ref.
$CdMoO_4$	$^{111}Cd/^{113}Cd$	<0.01	<0.03	14
CdI_2	$^{111}Cd/^{113}Cd$	<0.01	<0.03	15
α-SnF_2	^{119}Sn	0.221 ± 0.002	0.22	This work
Xe	^{129}Xe	0.024[a]	0.043	9
$TlClO_4$	^{205}Tl	0.5[b]	0.21	6
$TlNO_3$	$^{203}Tl/^{205}Tl$	1.4/1.4	0.57/0.58	5
$TlNO_2$	^{205}Tl	5[c]	2.1	7
$PbTiO_3$	^{207}Pb	0.90[d]	2.9	4
$PbCl_2$	^{207}Pb	1.18 ± 0.07	3.8	3
$Pb(NO_3)_2$	^{207}Pb	1.33 ± 0.03	4.3	1 and 2
$PbMoO_4$	^{207}Pb	2.25 ± 0.08	7.3	3

[a]Between 60 and 120 K.
[b]The value of A was estimated by numerical fitting of data points in Fig. 7 of Ref. 6.
[c]Raman relaxation process in addition to a relaxation mechanism due to NO_2- flips. The value of A was estimated by numerical fitting of a plotted curve in Fig. 1 of Ref. 7.
[d]The value of A was computed from Fig. 3 in Ref. 4.

The lack of a known value of Γ_0 for SnF_2 makes it difficult to calculate an expected magnitude for the spin-rotation relaxation rate constant A. However, agreement with the experimental value of $A=2.2\times10^{-7}$ s^{-1} K^{-2} may be obtained by choosing values for the various parameters that are within the ranges determined for similar compounds. For instance, $\Theta_D=200$ K, $\varepsilon=30$ nm^{-1},[8] and $v=5\times10^3$ m/s. For Γ_0 we choose 3×10^{-14} T s, which is close to the magnetorotation constant determined for ^{119}Sn in SnH_4 and $SnCl_4$ (2.8×10^{-14} and 3.0×10^{-14} T s, respectively).[8,36] With the substitutions $a=0.22$ nm, as discussed in Sec. I, and $m=53$ daltons from the f.u., an evaluation of the expression in Eq. (5) gives $A\approx4\times10^{-7}$ s^{-1} K^{-2}. This order-of-magnitude agreement demonstrates that the Raman process is most probably the dominant nuclear spin-lattice relaxation mechanism for ^{119}Sn in α-SnF_2 at lower temperatures.

The experimental value of A for SnF_2 is almost 1 order of magnitude smaller than the previously reported values of A for ^{207}Pb relaxation in several lead salts and for $^{203}Tl/^{205}Tl$ relaxation in several thallium salts, showing that this mechanism is less efficient for ^{119}Sn relaxation in SnF_2 (Table I).[1–7,9,15,16] For completeness, we note that this Raman process was not observed for $^{111}Cd/^{113}Cd$ relaxation in $CdMoO_4$ and CdI_2, implying that $A<10^{-8}$ s^{-1} K^{-2} for those two nuclear-spin species. A more direct insight into the relative efficiencies of the spin-rotation-mediated relaxation mechanism is obtained when the contribution of the magnetic properties of the nuclei is eliminated by division of A by γ^2 (for magnetogyric ratio γ). Comparison of the small set of values of A/γ^2 reported to date (fourth column in Table I) suggests that the sizes of the combined contributions of lattice vibrations and the spin-rotation interaction to the spin-lattice relaxation in the ionic lattices follow the trend $Cd \ll Sn < Tl < Pb$.

At higher temperatures, R shows a contribution from a thermally activated process described by a simple Arrhenius law with an effective activation energy of 70 ± 10 kJ mol^{-1}. This contribution to the observed relaxation rate likely arises from the dipole-dipole interaction between fixed ^{119}Sn spins and mobile ^{19}F spins. In principle, studies over a wide range of temperatures and NMR frequencies can often uniquely identify the process responsible for the relaxation. For example, NMR spectroscopy,[37,38] NMR relaxation,[39] and field-gradient diffusion studies[40] in LaF_3 identify different F sites in the crystal via anisotropic fluoride-ion dynamics. Measurements of the widths and asymmetries of ^{19}F, R, and R_ρ maxima (where R_ρ is the spin-lattice relaxation rate constant in the rotating frame) in BaF_2 have allowed determination of parameters that characterize the motion.[22,23] Translational motion in γ-$TiH_{1.63}$ gives a weak ($\omega^{1/2}$) frequency dependence to ^1H NMR relaxation (in the high-temperature fast-motion limit) from H^+ ions hopping among sites in the lattice.[41] Unfortunately, in the present case, the fact that the temperature range is limited on the low side by the dominance of the Raman mechanism below approximately 350 K and on the high side by the transition to the γ phase at 423 K limits the information that one can extract from analyzing a plot of R versus T. Though we cannot conclusively say that the high-temperature mechanism is due to fluoride-ion motion, it seems the most likely candidate.

IV. CONCLUSIONS

^{119}Sn NMR nuclear spin-lattice relaxation in α-SnF_2 is affected by two relaxation mechanisms in the range from 238 to 420 K. Below 350 K, relaxation is dominated by the nuclear spin-rotation Raman mechanism. This interaction is observed for a wide variety of spin-$\frac{1}{2}$ containing solids from ^{129}Xe in the van der Waals solid to heavier spin-$\frac{1}{2}$ nuclei such as ^{207}Pb and $^{203}Tl/^{205}Tl$ and now for ^{119}Sn. This mechanism is less effective for ^{119}Sn nuclei than for ^{207}Pb and $^{203}Tl/^{205}Tl$ by almost 1 order of magnitude but more effective for ^{119}Sn than for $^{111}Cd/^{113}Cd$, where it was not observed in careful relaxation measurements that indicate its strength is down by at least another order of magnitude from ^{119}Sn. These observations suggest a strong correlation with atomic mass but this needs further investigation since the quantum-mechanical details of the electronic structure may also play a significant role. Results reported for ^{109}Ag salts indicate very inefficient relaxation rates at room temperature, but the temperature dependence of the relaxation rate has not been reported. To our knowledge no relaxation experiments have been performed with the spin-$\frac{1}{2}$ nuclei ^{183}W, ^{187}Os, or ^{195}Pt (see Table I of Ref. 8).

At temperatures above 350 K, there is an additional thermally activated contribution to ^{119}Sn relaxation in α-SnF_2. We suggest that this results from the modulation of the unlike nuclear spin ^{119}Sn-^{19}F dipolar coupling by the motion of fluoride ions. The effective NMR activation energy derived from the temperature dependence of this contribution to the observed ^{119}Sn spin-lattice relaxation rate is comparable to activation energies measured in conduction experiments

where conduction is due to fluoride-ion motion. This high-temperature motion would be better studied in materials without a phase transition so a greater range of temperatures could be investigated.

ACKNOWLEDGMENTS

C.D. and P.A.B. acknowledge the support of the National Science Foundation under Grant Nos. CHE-0411790 and CHE-0411907.

[1] J. B. Grutzner, K. W. Stewart, R. E. Wasylishen, M. D. Lumsden, C. Dybowski, and P. A. Beckmann, J. Am. Chem. Soc. **123**, 7094 (2001).
[2] P. J. de Castro, C. A. Maher, R. L. Vold, and G. L. Hoatson, J. Chem. Phys. **128**, 052310 (2008).
[3] P. A. Beckmann, S. Bai, A. J. Vega, and C. Dybowski, Phys. Rev. B **74**, 214421 (2006).
[4] L.-S. Bouchard, A. O. Sushkov, D. Budker, J. J. Ford, and A. S. Lipton, Phys. Rev. A **77**, 022102 (2008).
[5] M. Villa and A. Avogadro, Phys. Status Solidi B **75**, 179 (1976).
[6] K. Morimoto, Phys. Rev. B **35**, 6608 (1987).
[7] Y. Furukawa and H. Kiriyama, Chem. Phys. Lett. **93**, 617 (1982).
[8] A. J. Vega, P. A. Beckmann, S. Bai, and C. Dybowski, Phys. Rev. B **74**, 214420 (2006).
[9] R. J. Fitzgerald, M. Gatzke, D. C. Fox, G. D. Cates, and W. Happer, Phys. Rev. B **59**, 8795 (1999).
[10] W. H. Flygare, *Molecular Structure and Dynamics* (Prentice-Hall, Englewood Cliffs, 1978).
[11] J. van Kranendonk, Physica (Amsterdam) **20**, 781 (1954).
[12] A. R. Lim and Se-Y. Jeong, J. Phys.: Condens. Matter **16**, 4403 (2004).
[13] A. Abragam, *The Principles of Nuclear Magnetism* (Clarendon, Oxford, 1961), p. 411.
[14] P. A. Beckmann, S. Bai, and C. Dybowski, Phys. Rev. B **71**, 012410 (2005).
[15] P. A. Beckmann, S. Bai, and C. Dybowski (unpublished).
[16] D. Ansel, J. Debuigne, G. Denes, J. Pannetier, and J. Lucas, Ber. Bunsenges. Phys. Chem **82**, 376 (1978).
[17] G. Denes, J. Solid State Chem. **37**, 16 (1981).
[18] R. C. McDonald, H. H. Hau, and K. Eriks, Inorg. Chem. **15**, 762 (1976).
[19] The inorganic structure database: Fachinformationszentrum Karlsruhe (FIZ) in Germany, and the National Institute of Standards and Technology (NIST) in the USA.
[20] M. Kumar, K. Yamada, T. Okuda, and S. S. Sekhon, Phys. Status Solidi B **239**, 432 (2003)
[21] N. I. Sorokin, Inorg. Mater. **40**, 989 (2004).
[22] D. Wolf, D. R. Figueroa, and J. H. Strange, Phys. Rev. B **15**, 2545 (1977).
[23] D. R. Figueroa, J. H. Strange, and D. Wolf, Phys. Rev. B **19**, 148 (1979).
[24] M. M. Ahmad, M. A. Hefni, A. H. Moharram, G. M. Shurit, K. Yamada, and T. Okuda, J. Phys.: Condens. Matter **15**, 5341 (2003).
[25] K. Yamada, M. M. Ahmad, Y. Ogiso, T. Okuda, J. Chikami, G. Miehe, H. Ehrenberg, and H. Fuess, Eur. Phys. J. B **40**, 167 (2004).
[26] S. Chaudhuri, F. Wang, and C. P. Grey, J. Am. Chem. Soc. **124**, 11746 (2002).
[27] V. Y. Kavun, E. B. Merkulov, and V. K. Goncharuk, Glass Phys. Chem. **30**, 320 (2004).
[28] G. Denes and E. Laou, Hyperfine Interact. **92**, 1013 (1994).
[29] R. K. Harris, E. D. Becker, S. M. Cabral de Menezes, R. Goodfellow, and P. Granger, Pure Appl. Chem. **73**, 1795 (2001).
[30] P. Amornsakchai, D. C. Apperley, R. K. Harris, P. Hodgkinson, and P. C. Waterfield, Solid State Nucl. Magn. Reson. **26**, 160 (2004).
[31] G. Neue, C. Dybowski, M. L. Smith, M. A. Hepp, and D. L. Perry, Solid State Nucl. Magn. Reson. **6**, 241 (1996).
[32] R. W. Martin and K. W. Zilm, J. Magn. Reson. **168**, 202 (2004).
[33] A. L. Van Geet, Anal. Chem. **42**, 679 (1970).
[34] A. L. Van Geet, Anal. Chem. **40**, 2227 (1968).
[35] P. A. Beckmann and C. Dybowski, J. Magn. Reson. **146**, 379 (2000).
[36] A. Laaksonen and R. E. Wasylishen, J. Am. Chem. Soc. **117**, 392 (1995).
[37] D. Kruk, O. Lips, P. Gumann, A. Privalov, and F. Fujara, J. Phys.: Condens. Matter **18**, 1725 (2006).
[38] A. F. Privalov, A. Cenian, F. Fujara, H. Gabriel, I. V. Murin, and H.-M. Vieth, J. Phys.: Condens. Matter **9**, 9275 (1997).
[39] A. F. Privalov, O. Lips, and F. Fujara, J. Phys.: Condens. Matter **14**, 4515 (2002).
[40] V. V. Sinitsyn, O. Lips, A. F. Privalov, F. Fujara, and I. V. Murin, J. Phys. Chem. Solids **64**, 1201 (2003).
[41] N. Salibi and R. M. Cotts, Phys. Rev. B **27**, 2625 (1983).